

# EXPERIMENTAL APPARATUS FOR THE DETERMINATION OF THERMAL CONDUCTIVITY AND HUMIDITY IN BUILDING MATERIALS BY MEANS OF ELECTRICAL PERMITTIVITY MEASUREMENTS

Alessio Perinelli<sup>a</sup>, Francesco Finotti<sup>b</sup>, Arnaldo M. Tonelli<sup>b</sup>, Leonardo Ricci<sup>a</sup>, Rossano Albatici<sup>c\*</sup>

<sup>a</sup> *Department of Physics, University of Trento, via Sommarive 14, Trento, 38123, Italy*

<sup>b</sup> *Geo.Ti.La, corso Bettini 58, Rovereto, 38060, Italy*

<sup>c</sup> *DICAM, Department of Civil Environmental and Mechanical Engineering, University of Trento, via Mesiano 77, Trento, 38123, Italy*

---

## Highlights

Relationship between thermal conductivity and electrical permittivity for different building materials is defined. A novel test apparatus for laboratory activity has been designed and realized based on a special capacitive sensor where the material sample act as dielectric. The first measurement approach has been refined by considering parallel measurements consisting in the comparison of the frequency of two oscillators. Electrical permittivity shows to be well correlated to the moisture content and variation of the material under investigation.

---

## Abstract

The on-site measurement of the thermal properties of existing building envelopes is of utmost importance to fairly accurately calculate the thermal loss by transmission to the outside environment and so to define the building overall energy performance. This paper presents a preliminary investigation concerning the use of a new indirect method for measuring the thermal characteristics of building materials throughout the year based on the analysis of the material electrical properties. The main goal is to identify a relationship between thermal transmittance, moisture content and electrical impedance through relative electrical permittivity measurements.

---

## Keywords

Thermal conductivity, Moisture content, Electrical permittivity, Building materials

---

## 1. INTRODUCTION

The Directive 2010/31/EU of the European Parliament and of the Council of 19 May 2010 on the energy performance of buildings [1], recently integrated and updated with the Directive (EU) 2018/844 [2] and with the Italian national laws, including the Decree 26/06/2015 [3], stressed the necessity to decrease heating and cooling energy consumptions for both existing and new buildings. Despite that, there is still a lack of diagnostic tools for verifying the real thermal behaviour of the building envelope. To date, the only references are represented by the International Standard ISO 9869-1:2015 [5], concerning the heat flow meter method, and the ISO 9869-2:2018 [6] that describes the method for measuring the thermal resistance and thermal transmittance of opaque building elements with a thermal capacity lower than  $30 \text{ kJ/m}^2\text{K}$  on existing buildings with frame structure dwellings, using an infrared (IR) camera. The authors have already probed the possibility of using in-situ thermography in order to evaluate with good approximation the thermal transmittances of opaque building components [6-8]. However, there are still some limitations in this field due essentially to the

---

\* Corresponding author. Tel.: +39-0461-282622; fax: +39-0461-282672; e-mail: rossano.albatici@unitn.it

specific boundary conditions needed. As confirmed by other researches [9-10], a constant thermal gradient of 10-15°C between internal and external environment is necessary, both before and after the measurement. Therefore, an investigation about the potential relationship between thermal transmittance and electrical impedance of multi-layered panels made of typical building materials has been undertaken. The purpose was to indirectly understand the thermal behaviour of these panels through a rapid, non-destructive and repeatable procedure, without being influenced by outdoor environment conditions and so repeatable throughout the year, at any time. As far as the authors know, the only previous attempt to follow this path was made in 1938 by J. Stuart Johnson [12], within a laboratory environment and considering only components made of brick. The research highlighted some problematic issues such as the need to use high frequency alternating current and the difficulty in reducing potential noises produced by measurement equipment. Moreover, the results, which frequently depended on uncontrollable a priori causes, were hard to read.

For this reason, we decided to pursue a more well-structured step-by-step process of increasing complexity. The starting point was the analysis of samples of homogeneous material, undertaken under laboratory controlled conditions, in order to measure materials permittivity and to compare it with thermal conductivity values. Permittivity is correlated to the capacitive component of the samples and to their electrical impedance too. This procedure might successfully be used also to determine the humidity of the material.

## **2. METHODOLOGY**

The initial assumption is that the samples under investigation are made of material which can be considered ideal insulator (infinite electric resistance) with null inductive component. Proceeding this way, the impedance associated to the specific sample is exclusively a result of the material dielectric properties. The fact that most of the good electrical conductor materials are also efficient thermal conductors and that bad electrical conductors are characterized by a low thermal conductivity, supports this approach.

Four square panel having a side length of 20cm and 2cm thick, respectively made of fir wood, glass, polystyrene and concrete are examined. Each sample consists of a single material and can be consequently considered as homogenous and isotropic. Thermal properties have been previously defined by the Industrial Engineering Department of the University of Padua<sup>1</sup> through the hot disk method, in order to obtain values which can be related to electrical measurement results.

### ***2.1 Measurement equipment***

The apparatus for measuring impedance (Fig. 1) is composed of two square metal plates having a side length of 30cm which are placed concentrically and locked with four nylon rails. Pressing on the sample faces, a large condenser is formed, with the sample working as a dielectric. The circuitry is incorporated in a metal box directly welded on the plate which is grounded. Thanks to two BNC connectors, it is possible to operate the circuitry and immediately read the results.

---

<sup>1</sup> The authors thank Dr. Manuela Campanale and Dr. Lorenzo Moro of the University of Padua for their kind collaboration

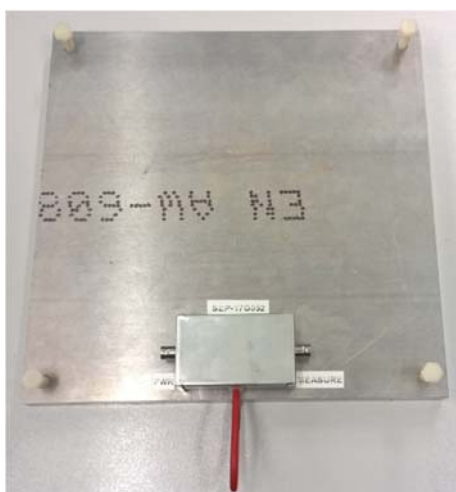


Figure 1. The apparatus with the electric circuit incorporated in the metal box

The measurement of the resistive component of impedance of the apparatus is quite complicated due to several reasons like, firstly, the difficulty to create a good electrical contact between the plates and the sample. This led to consider the sensor as an exclusively capacitive element, in order to weigh the sample dielectric characteristics. Considering the circuitry, the sensor can be seen as a combination of condensers ( $C_1$ ,  $C_2$ ,  $C_x$  and  $C_b$ ) positioned as shown in Fig. 2a, each one associated to a portion of the volume between the two plates. Eq.1 provides the total capacity of the sensor  $C_{tot}$ .

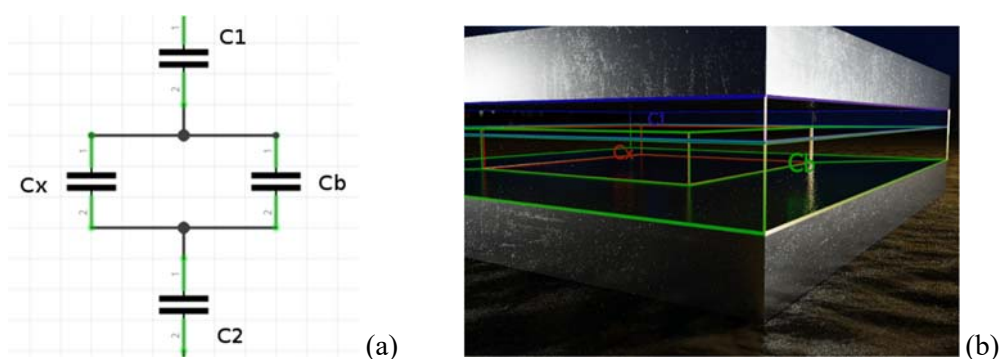


Figure 2. The circuitry associated to the apparatus (a), subdivision of the volume between the two plates of the equipment (b)

The portions of the volume associated to  $C_1$ ,  $C_2$ ,  $C_x$  and  $C_b$  (Fig. 2b) are:

- the volume determined by the dimensions of the sample located in the centre of the sensor, which contributes to the total capacity of the sensor itself with  $C_x$ ;
- "edge volume", i.e. the volume with the same height as the sample and with the base equal to the difference between the surface occupied by the samples and the plate area, which contributes with  $C_b$ ;
- the volume identified by the air layer which separates the upper plate and the aforementioned volumes, which contributes with  $C_1$ ;
- the volume identified by the air layer which separates the lower plate and the first two depicted volumes, which contributes with  $C_2$ .

The total sensor capacity  $C_{tot}$  is equal to:

$$1/C_{tot} = 1/C_1 + 1/C_2 + 1/(C_x + C_b) \quad (1)$$

$C_2$  can be considered infinite since the sample rests on the lower plate. Hence:

$$C_{tot} = [C_1 (C_x + C_b)] / [(C_x + C_b + C_1)] = (C_x + C_b) / [1 + (C_x + C_b) / C_1] \quad (2)$$

If  $C_1$  is much higher than the sum of  $C_x$  and  $C_b$ , i.e. if the upper plate is very close to the upper face of the sample, then:

$$C_{tot} = C_x + C_b \quad (3)$$

Referring to the circuitry,  $Z_s$  impedance associated to the sensor is equal to:

$$Z_s = i / (\omega C_{tot}) \quad (4)$$

with  $i$  representing the intensity of the circuit current.

The circuitry built for this study, shown in Fig.3, is a classical divider circuit composed of a resistor  $R$  and the sensor  $Z_s$  described above. A sinusoidal signal with potential difference  $V_{in}$  supplies the circuit and is taken as a reference by a 'lock-in' tool to detect phase signals. The signal at the output of the  $V_{out}$  circuit is thus monitored to measure amplitude  $A$  and phase difference  $\phi$ . The  $C_{tot}$  capacity of the circuitry can therefore be derived as:

$$C_{tot} = (\sqrt{(a^2 - 2A \cos \phi + 1)}) / \omega R_a = (\sqrt{(a^2 - 2A \cos \phi + 1)}) / 2\pi F R A \quad (5)$$

where  $F$  is the frequency in Hertz to which the circuitry is powered.

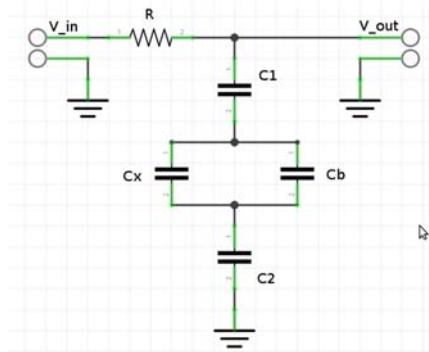


Figure 3. Circuit diagram

## 2.2 Measurement procedure – first phase

During the first phase of the experimentation, in order to test the assessed methodology, only one sensor is used and the measurement have been repeated twice, with and without sample. The distance between the two plates, which are close enough to suppose  $C_1 \gg C_x + C_b$ , is maintained, using some shims to extract the sample from the equipment. Hence, after positioning the sample in the centre of the sensor, amplitude  $A$  and phase difference  $\phi$  are measured at difference frequencies. As mentioned before, measurements are repeated keeping the same configuration and without the sample (only air is present). Following this methodology, the only capacitive component that influences  $C_{tot}$  values is  $C_x$ .

When the sample  $c$  is present:

$$C_x = C_c \quad (6)$$

When the sample is missing and his volume is filled by air  $a$ :

$$C_x = C_a \quad (7)$$

Considering the difference between the total capacities of the sensor  $Z_s$  with and without the sample, the dependence on the edge capacity  $C_b$  is eliminated. Using (3):

$$\Delta C_{\text{tot}} = C_c - C_a \quad (8)$$

The volume identified by  $C_x$  has the size of the sample, surface  $S$  and thickness  $l$ . The capacities  $C_c$  and  $C_a$  are respectively:

$$C_c = (\epsilon_0 \epsilon_{r(\text{sample})}) * S / l \quad (9)$$

$$C_a = (\epsilon_0 \epsilon_{r(\text{air})}) * S / l \cong \epsilon_0 * S / l \quad (10)$$

where  $\epsilon_0$  is the dielectric constant of the vacuum (vacuum permittivity).

Since the relative dielectric constant of air  $\epsilon_{r(\text{air})} = 1.0006 \cong 1$  it is possible to replace (10) in (9) and approximate  $C_c$  as follows:

$$C_c = C_a \epsilon_r = C_a (\epsilon_r - 1) + C_a \quad (11)$$

where  $\epsilon_r$  is the relative permittivity of the sample.

Consequently, by replacing (11) in (8), the difference in measured capacity  $\Delta C_{\text{tot}}$  results:

$$\Delta C_{\text{tot}} = C_a (\epsilon_r - 1) \quad (12)$$

from which it is possible to derive  $\epsilon_r$  as:

$$\epsilon_r = (\Delta C_{\text{tot}}) / C_a + 1 \quad (13)$$

The resistance  $R$  of the circuit was chosen equal to  $1M\Omega$  in order to maximize its sensitivity. To avoid any external interference during the measurements the equipment was placed in a Faraday cage (Fig. 4).

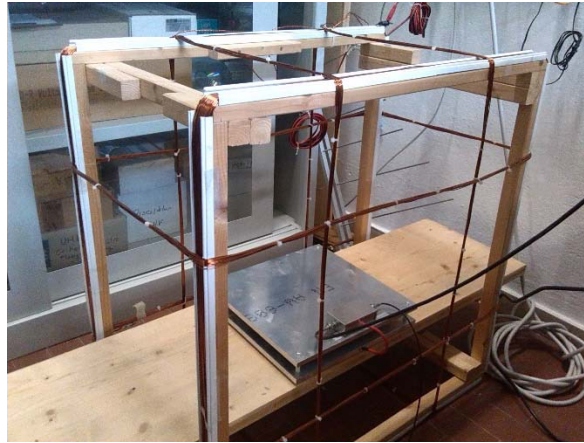


Figure 4. The apparatus placed in a Faraday cage

The circuit was powered at different frequencies with the function generator provided inside the Stanford Research Systems lock-in tool, model SR830 DSP. The measurements of the amplitude of the input voltage  $V_{\text{in}}$  and of the output voltage  $V_{\text{out}}$ , those of the phase shift of the input signal with respect to the synchronization signal  $\phi_0$  and the correspondent for the output signal  $\phi_{\text{out}}$ , were collected.

The frequencies at which measurements were made are in the range  $300 \div 1500\text{Hz}$  at  $100\text{Hz}$  intervals and the amplitude of the input signal has been set at  $1\text{V}$  peak-to-peak. After estimating  $C_a$  as described in (10), the  $C_{\text{tot}}$  total capacity measurements of the equipment in the configuration with and without samples were collected. Finally, the relative permittivity  $\epsilon_r$  was calculated with (13).

### 2.3 Measurement procedure – second phase

During the second phase, two in-parallel measurement sensors have been used in order to collect data with and without the sample simultaneously (Fig. 5).

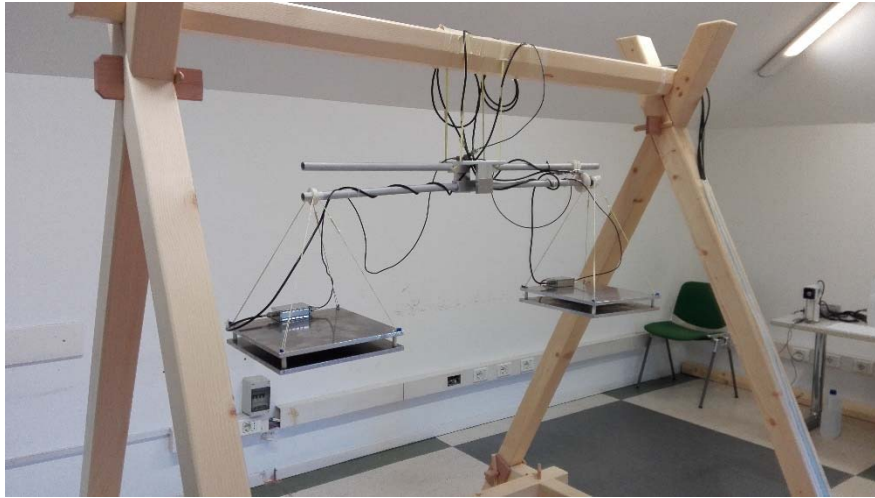


Figure 5. The new apparatus made of two in-parallel measurement sensors

This process allows to remove every uncertainty due to measurement repetitions, in particular those correlated to boundary condition variations (environment temperature and humidity). It is also possible to test a sample and a referenced capacity at the same time.

Even the sensor and the measurement procedure have been improved. The instrumentation is now composed of two identical capacitors, both made of two square aluminium plates having a side length of 30cm, distant 3cm one from the other and fixed together using spacers and plastic screws. The capacitors are located on a rocker arm with equal sides hanging on a wooden structure. Each of them is the capacitive element of a relaxation oscillator. By measuring the period of the oscillators, it is possible to estimate the dielectric constant of the sample located in the capacitor. In order to improve the electromagnetic isolation of the sensor (which in the previous equipment was guaranteed by the Faraday cage), a third thinner plate is fixed below the pair of plates and grounded as the upper plate. Fig. 6 shows the new operating system.

Since it is a time-measurement (that is, of the period of the oscillators), this system is more accurate than the previous one, in which the detection was carried out in phase by means of a lock-in amplifier.

In order to compare the dielectric constant measurement  $\epsilon_r$  of the sample with the time variation of its water content, the weight of the latter is measured simultaneously with the oscillator periods. To this end, the two capacitors constitute the plates of a scale with equal arms. A load cell is attached to one of the two arms to measure the weight difference between the two arms. The load cell consists of a Wheatstone bridge read by an ADC (Analog to Digital Converter). The period measurement is undertaken using an FPGA (Field Programmable Gate Array), measuring the time  $T_N$  each oscillator takes to perform  $N = 1280$  oscillations and then calculating the average period  $T_N / N$ . Since the oscillation frequency of the oscillators with (or without) the sample is about 3.5 kHz (2.3 kHz), the acquisition takes about half a second. The 24 bits produced by the ADC that reads the load cell are acquired by the same FPGA together with the measurement of the periods.

The data are transmitted from the FPGA to a computer as soon as they are available. The system has been properly calibrated both in weight and in capacitance. During acquisition, the temperature and relative humidity of the testing environment are recorded by an independent system every 5 minutes.

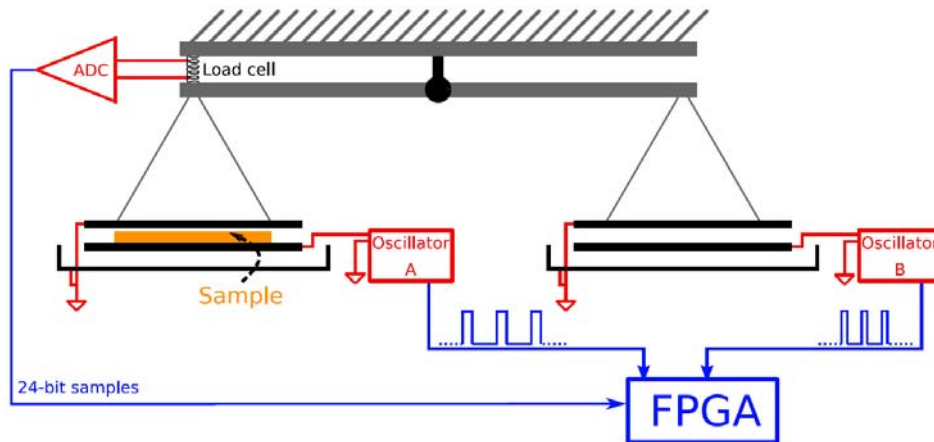


Figure 6. The operating principle of the new measuring system

#### 4. RESULTATS AND DISCUSSION

For the sake of brevity, the graphs of the permittivity  $\epsilon_r$  of the four samples as a function of the frequency in Hertz (Fig. 7), measured with the first instrumentation, are reported below.

Considering concrete, two tests were undertaken, with dry and wet (after three days of bathing in a container full of water) test specimens.

It should be noted that basically the values are constant with the variation of the frequency considered. The trends found were interpolated with a constant function to find the reference value of  $\epsilon_r$  for each investigated material.

As mentioned above, it is reasonable to think that the resistive and inductive components of the impedance associated with the samples tend respectively to infinity ( $R_c \rightarrow \infty$ ) and zero ( $L_c \rightarrow 0$ ) because of the nature of the materials itself of which they are composed. The approximation made for this preliminary analysis is therefore to consider the materials as if they had only capacitive properties

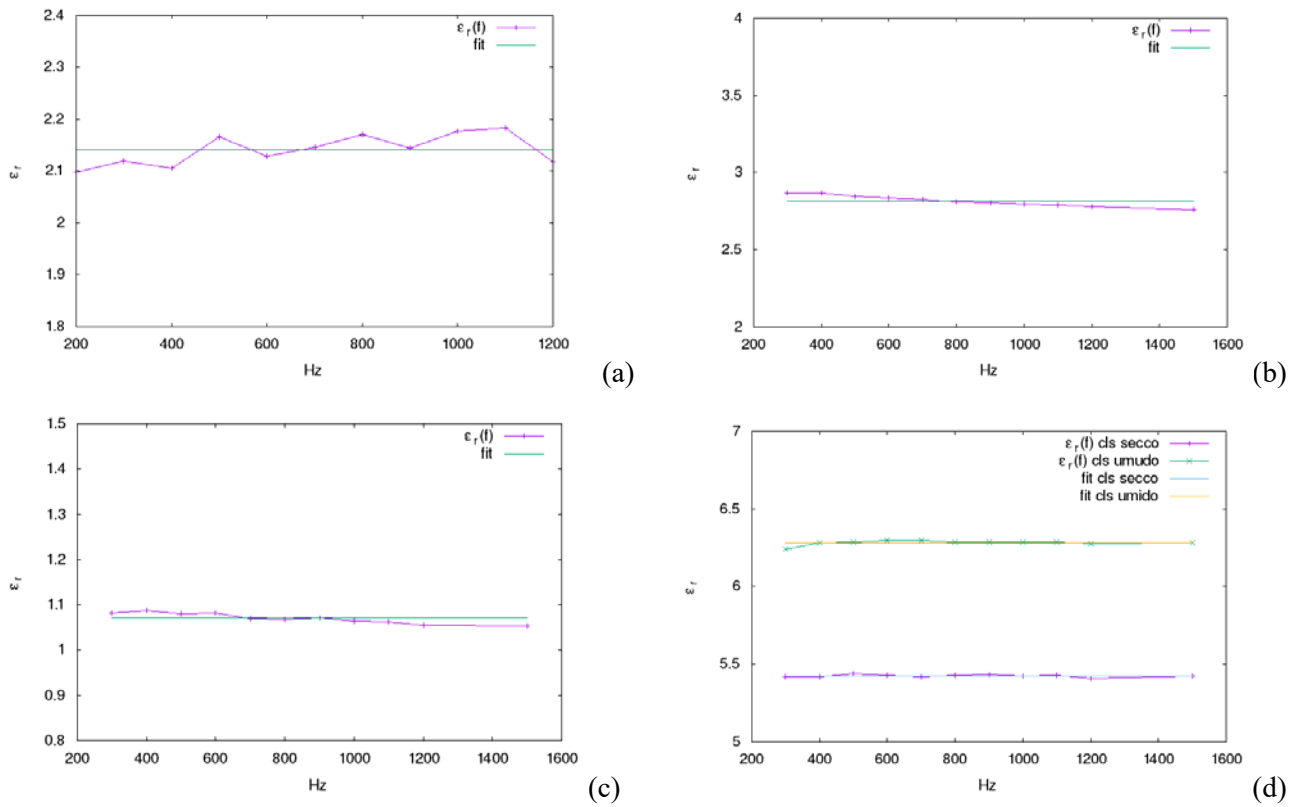


Figure 7. Plot of permittivity  $\epsilon_r$  of the four samples according to the frequency considered: (a) fir wood, (b) glass, (c) polystyrene, (d) dry and moist concrete (upper curve).

The following table (Tab. 1) shows the reference permittivity values obtained for the different samples, with the relative thermal conductivity values measured in laboratory.

sample	$\lambda$ [W/m <sup>2</sup> K]	$\epsilon_r$
polystyrene	0.0348	$1.070 \pm 0.003$
fir wood	0.1718	$2.141 \pm 0.009$
glass	1.0240	$2.82 \pm 0.01$
dry concrete	1.6070	$5.425 \pm 0.002$
moist concrete	---	$6.283 \pm 0.004$

Table 1. Thermal conductivity and electrical permittivity of the four materials considered

It's possible to notice that  $\epsilon_r$  of the polystyrene is very close to that of the air, since the volume of polystyrene consists mainly of air. In a similar way, comparing  $\epsilon_r$  of dry and wet concrete, the presence of water contributes significantly to the increase in permittivity. Although the number of samples is insufficient to draw definitive conclusions, a correlation between the thermal and electrical properties of the materials is noted, as highlighted in the graph in Fig. 8

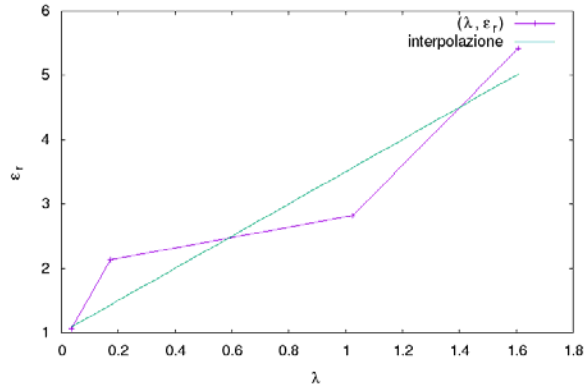


Figure 8. The correlation between thermal conductivity ( $\lambda$ ) and relative electrical permittivity ( $\epsilon_r$ ) of the samples

We chose to interpolate the graph with a linear function of angular coefficient (or proportionality constant between  $\lambda$  and  $\epsilon_r$ )  $k_\lambda$  and intercept  $q = 1$ . The latter value is defined since the thermal conductivity of the vacuum must be zero. The ratio between thermal conductivity and electrical permittivity is therefore equal to:

$$\lambda = (\epsilon_r - 1)/k_\lambda = k_\lambda (\epsilon_r - 1) \quad (14)$$

where

$$k_\lambda = 0.40 \pm 0.05 \text{ [W/mK]}$$

The equipment composed of the two sensors and the rocker arm has been used to correlate permittivity and moisture content of the material. For this purpose, a series of ever more refined measurements have been made on wet concrete, evaluating the variation of its electrical properties during its drying.

The wet sample is initially placed in one of the two capacities. The period of the two oscillators and the output of the load cell are measured continuously for several days, necessary for the complete evaporation of the water and its equilibrium with the surrounding environment. Fig. 9 shows some preliminary results collected in 10 days. Data are presented in terms of water mass and dielectric constant of the sample  $\epsilon_r$ . The raw data, i.e. the period values and the output of the ADC, were processed by applying a running average with a subset of 100 samples.

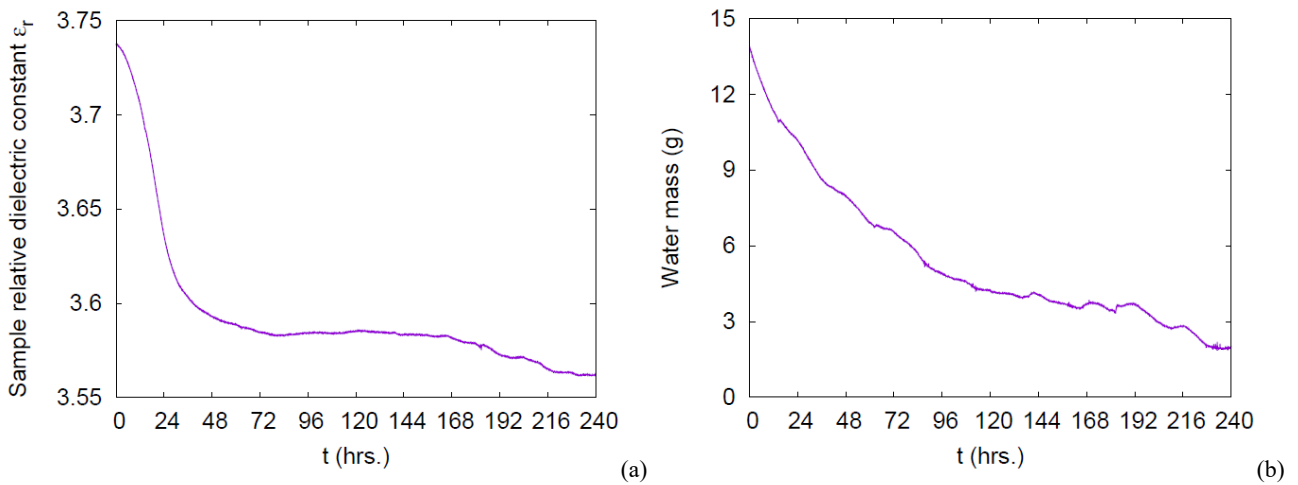


Figure 9. The results of a single 10-days acquisition. (a) Relative dielectric constant  $\epsilon_r$  of the sample as a function of time. (b) Mass of water contained in the sample as a function of time

The preliminary results show that the equipment is promising and represents an improvement of the measurement method used before. Both the equipment and the analysis are being further developed. For example, measurements can be corrected for ambient temperature and humidity. It has already been observed that the fluctuations of the measured weight value, visible in particular for  $t = 144 \div 240$  hrs in Fig. 9b, are consistent with the fluctuations of the temperature recorded in the room, not reported here. Therefore, in a future improvement of the analysis the weight data will be corrected considering the environment temperature. Moreover, the estimation of the dielectric constant of the sample reported in Fig. 9a is comparable, but lower, than the nominal value of concrete (4.5, while with the first equipment an average value equal to 5.4 was recorded, see Fig. 7c). The discrepancy is caused by an inaccurate estimation of the sample volume: although the sample has an irregular thickness, the porosity of the sample itself has not been evaluated. In the future these effects will be considered and it will be possible to obtain more reliable evaluations of the dielectric constant.

## 5. CONCLUSIONS

The research in this article shows a relationship between thermal conductivity and electrical permittivity of four tested samples, according to a linear law with a defined slope coefficient. A relatively simple instrumentation for its measurement can be easily realized. Similarly, by appropriately refining the measurement, it is also possible to relate the electrical permittivity of the samples with their water content, monitoring the trend over time. What is proposed, however, is a first step in a broader and more complex research. The possibility of defining the thermal transmittance of the building envelope by means of a law that correlates it to the electrical properties of the envelope itself should be investigated more. Further developments must consider the resistive and inductive components of the samples too, in order to fully assess their impedance. The number of samples considered must also be increased to prove the relationship between the two quantities considered (even if not necessarily linear), even in the case of multi-material, stratified or mixed samples. Finally, a measuring apparatus that can be easily transportable and used on site under real conditions should be improved.

## 6. REFERENCES

- [1] Directive 2010/31/EU of the European Parliament and of the Council, *on the energy performance of buildings (recast)*. European Union: Brussels, 2010, <<https://eur-lex.europa.eu>>. (Last viewed: 5/5/2019)
- [2] Directive 2018/844/EU of the European Parliament and of the Council, *amending Directive 2010/31/EU on the energy performance of buildings and Directive 2012/27/EU on energy efficiency*. European Union: Brussels, 2018, <<https://eur-lex.europa.eu>>. (Last viewed: 5/5/2019)
- [3] Interministerial Decree 26 June 2015, *Application of energy performance calculation methodologies and definition of minimum prescription and requirements for buildings*, 2015, <<http://www.sviluppoeconomico.gov.it/index.php/it/>>. (Last viewed: 5/5/2019)
- [4] UNI ISO 9869-1:2015, *Thermal insulation -- Building elements -- In-situ measurement of thermal resistance and thermal transmittance - Part 1: Heat flow meter method*. Milan: Ente Italiano di Normazione (UNI); 2015
- [5] ISO 9869-2:2018, *Thermal insulation -- Building elements -- In-situ measurement of thermal resistance and thermal transmittance Infrared method for frame structure dwelling*. Brussels: European Committee for Standardization (CEN); 2018
- [6] Albatici R.; Tonelli A.M., Infrared thermovision technique for the assessment of thermal transmittance value of opaque building elements on site. *Energy and Buildings*, 42 (2010), p. 2177–2183.
- [7] Albatici R.; Passerini F.; Tonelli A.M.; Gialanella S., Assessment of the thermal emissivity value of building materials using an infrared thermovision technique emissometer. *Energy& Buildings*, 66 (2013), p. 33–40.

- [8] Albatici R.; Tonelli A.M.; Chiogna M., A comprehensive experimental approach for the validation of quantitative infrared thermography in the evaluation of building thermal transmittance. *Applied Energy*, 141 (2015), p. 218–228.
- [9] Fokaides P.A.; Kalogirou S.A., Application of infrared thermography for the determination of the overall heat transfer coefficient (U-value) in building envelopes. *Applied Energy*, 88 (2011), p. 4358–65.
- [10] Dall’O G.; Sarto L.; Panza A., Infrared screening of residential buildings for energy audit purposes: results of a field test. *Energies*, 6 (2013), p. 3859–78.
- [11] Albatici R.; Cristofolini M.; Tonelli A.M., Comparison between thermal transmittance and electrical impedance in building walls. In: *Proceeding of the 40th IAHS World Congress on Housing - Sustainable Housing Construction*. ITeCons, Coimbra, Portugal. 2014, pp. 1-10.
- [12] Stuart Johnson J., Correlation of electrical and thermal properties of building brick. *Journal of the American Ceramic Society*, 21 (1928), n. 3, p. 79-85.